LAWRENCE LIVERMORE NATIONAL LABORATORY

LLNL-JRNL-520620

Prompt Energy Distribution of 235U(n,f)gamma at Bombarding Energies of 1 to 20 MeV

E. Kwan, C. Y. Wu, R. C. Haight, H. Y. Lee, T. A. Bredeweg, A. Chyzh, M. Devlin, N. Fotiades, J. M. Gostic, R. A. Henderson, M. Jandel, A. Laptev, R. O. Nelson, J. M. O Donnell, B. A. Perdue, T. N. Taddeucci, J. L. Ullmann, S. A. Wender

December 16, 2011

Nuclear Instruments and Methods A

Disclaimer

This document was prepared as an account of work sponsored by an agency of the United States government. Neither the United States government nor Lawrence Livermore National Security, LLC, nor any of their employees makes any warranty, expressed or implied, or assumes any legal liability or responsibility for the accuracy, completeness, or usefulness of any information, apparatus, product, or process disclosed, or represents that its use would not infringe privately owned rights. Reference herein to any specific commercial product, process, or service by trade name, trademark, manufacturer, or otherwise does not necessarily constitute or imply its endorsement, recommendation, or favoring by the United States government or Lawrence Livermore National Security, LLC. The views and opinions of authors expressed herein do not necessarily state or reflect those of the United States government or Lawrence Livermore National Security, LLC, and shall not be used for advertising or product endorsement purposes.

*Manuscript

Prompt Energy Distribution of ^{235}U(n,f)γ at Bombarding Energies of 1 to 20 MeV

E. Kwan[a], C. Y. Wu[a], R. C. Haight[b], H. Y. Lee[b], T. A. Bredeweg[b], A. Chyzh[a], M. Devlin[b], N. Fotiades[b], J. M. Gostic[a], R. A. Henderson[a], M. Jandel[b], A. Laptev[b], R. O. Nelson[b], J. M. O'Donnell[b], B. A. Perdue[b], T. N. Taddeucci[b], J. L. Ullmann[b], S. A. Wender[b]

[a] *Lawrence Livermore National Laboratory, Livermore, CA 94551 USA*
[b] *Los Alamos National Laboratory, Los Alamos, NM 87545 USA*

Abstract

The distributions of prompt γ rays from the spontaneous fission of ^{252}Cf and neutron-induced fission of ^{235}U were measured up to $\sim$4 MeV using a liquid scintillator array. The unfolding of measured fission γ rays are presented using the Single Value Decomposition and iterative Bayesian methods. General agreement was found with comparisons made with previous measurements. The energy dependence of the prompt γ-ray distributions for the spontaneous fission of ^{252}Cf and the neutron-induced fission of ^{235}U from bombarding energies of 1-2, 5-10, and 10-20 MeV were found to be almost identical in the γ-ray energy region 1 to 4 MeV.

Keywords: Uranium-235, Neutron-induced fission, Liquid scintillator, Gas counter, Prompt γ-ray spectra

1. Introduction

Investigations into the observables in fission are needed to improve our understanding of the fission process and the products released. Accurate data in the energy of the emitted particles from fission, such as neutrons and γ rays, their angular distributions, and production cross sections are needed for radiation transport calculations for a wide range of applied programs. Such information is important in analyzing nuclear energy designs and safeguards scenarios. For example, the energies of the neutrons, γ rays and fragments produced from the fission process will essentially be deposited within the surrounding materials in the form of heat. Although the majority of available energy created from the fission event will be in the form of kinetic energy of the recoiling fission fragments, approximately 10% of the total energy in a core of the reactor is released in form of prompt, delayed and radiative capture γ rays [1]. In fast breeder reactors, heating due to γ rays accounts for $\sim$13% of the total energy and may be the dominate contributor of the heating in the sub-assemblies and shielding [2]. Knowledge of the shapes of the energy distributions is necessary to design

Email address: kwan1@llnl.gov (E. Kwan)

proper shielding and cooling systems, and characteristics of photon heating, mainly due to the prompt γ rays, are needed to reduce the uncertainties of γ heating from 15% [3] to the requested one of less than 7.5% [4].

Experimental data are also necessary to test the accuracy of the predictions from nuclear reaction codes such as TALYS [5] and EMPIRE [6]. The neutron-induced fission cross sections and fission yields for the actinides have been studied since the 1950's, see for example Ref. [7]. While significant work has been done to measure the neutron-induced fission cross section of ^{235}U and the prompt neutron multiplicity ($\overline{\nu_p}$), large uncertainties in the prompt neutron spectrum still exist at thermal incident energies [8]. In the case of fission of ^{235}U induced by neutrons above thermal, experimental data on the prompt neutron distributions also exist for neutron incident energies from 0.4 to 200 MeV [9], below approximately 8.0 MeV [10, 11] and at 14.7 MeV [12]. Theoretical models predict that there should be little dependence of the measured shapes of the neutron distributions versus the incident neutron energy [13]. However, comparisons with the experimental data at thermal and 0.5 MeV show variations as large as 15%. For the prompt γ-ray distributions, there is even less experimental information available. In fact, there is only a handful of data available for any actinide showing the γ-ray distribution. Verbinski *et al.* [14] measured the shape of the γ-ray spectrum at thermal bombarding energy and Drake measured the distributions using 1-, 2- [15], and 5- to 8-MeV [16] neutrons.

The neutron source at the Los Alamos Neutron Science Center (LANSCE) provides a pulsed neutron distribution with neutron energies ranging from hundreds of keV to several hundreds of MeV at the Weapons Neutron Research facility (WNR) by spallation of a 800-MeV proton beam on a thick tungsten target. The resulting continuum neutron distribution enables us to measure simultaneously the prompt neutron and γ-ray spectra as a function of incident energies in a single experiment. The feasibility of exacting information about the neutron and γ-ray distributions by using the same detector opens up the opportunity to study γ-neutron correlations while simultaneously reducing the amount of scattering material that can distort the low energy part of the neutron spectrum. The prompt γ-ray and neutron distributions from neutron-induced fission of ^{235}U were obtained simultaneously at LANSCE and analyzed separately. The measured prompt γ-ray spectra along with the unfolded ones deduced using iterative Bayesian and Single Value Decomposition techniques are presented and compared with available data.

2. Experiment

The present work was fielded at the WNR facility using the FIGARO neutron detector array [17] to measure the distributions of the prompt neutrons and γ rays emitted from fission. The array held seventeen Eljen EJ301 organic liquid scintillators each with active volumes of 613.6 cm^3 (12.5 cm in diameter, 5.0 cm in depth). The detectors were positioned approximately 1 meter away from the center of the target position yielding an angular coverage from 42° to 125° in the lab frame. Of the 17 scintillators, only six detectors with the best pulse-height distributions were chosen for the analysis. The particles detected by the liquid scintillators were identified using the double time-of-flight (TOF) technique, which measures the time difference between the source pulse and the fission event as well as between the fission event and the neutron detectors. The source pulse time was determined by an electrical pick-off of the proton beam from the accelerator.

Fission events were detected by Parallel Plate Avalanche Counter ($PPAC$), which was fabricated at the Lawrence Livermore National Laboratory with a design that minimized the amount of structural material that can scatter neutrons [18]. A counter contained 10 foils of ^{235}U with a total mass of approximately 113 mg. Uranium-235 enriched to 99.91% was deposited on both sides of a 4 cm in diameter 3-μm thick titanium backing foil [19]. Two 1.4-μm thick double-sided aluminized mylar foils glued to G-10 rings sandwiched the target and were grounded to serve as the cathode for the avalanche counter. The anodes positioned 3 mm away from the cathode consisted of the same type of aluminized mylar foils. The signals from the anodes on either side of the target were coupled together thus reducing the number of required feedthroughs. Platinum foils of 5-μm thickness were placed on either side of the stack holding the anodes and cathodes to stop the fission fragments and α's from interfering with the neighboring anodes-cathode stacks. A similar design was used for the second $PPAC$. In this case, the PPAC contained a single foil with a deposit of ^{252}Cf. This foil had a specific activity of approximately 2 μCi and was placed at the center position in the fission detector.

The $PPAC$'s were used to detect the fission fragments and were biased to $\sim$+400 V was operated using $\sim$4 torr of isobutane. No information about the directions and masses of the fragments was obtainable with these counters. The fast timing of these particular counters resulted in an approximately 1-ns time resolution for the photon-induced fission peak in the time-of-flight spectrum obtained from the time difference of the counter relative to beam pick-off of the proton LINAC. The fission pulse height versus time of flight measured by a single liquid scintillator is shown in Fig. 1. The prompt γ rays concentrated at around 3 ns in the time-of-flight spectrum are clearly resolved from the prompt neutrons that occur more than 20 ns later.

The fission gamma rays can also be differentiated from fission neutrons by gating on the fast and slow components of the scintillation pulse. The fraction of the light in the tail of the pulse (i.e. the slow component), which typically depends on the rate of energy loss, compared to the fast component is a function of the particle type. In the current work, the gate for the fast component was set to measure the first $\sim$25 ns of the pulse and the gate for slow component was set to measure $\sim$150 ns of the tail. Shown in Fig. 2 is the pulse height distribution from the neutron-induced fission of ^{235}U for the slow vs. the fast components of the scintillation light measured by a single liquid scintillator. The particles with the largest energy lost per unit length (dE/dX), i.e. the recoiling protons from n-p scattering, are concentrated predominately along the diagonal of the figure while the events due to the γ-ray interactions are in the upper left part of the

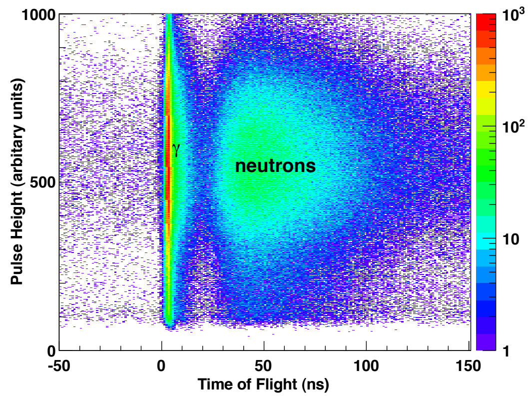

Figure 1: The intensity distribution of the fission fragment pulse height vs. the time-of-flight of the emitted particles from the PPAC to the neutron array.

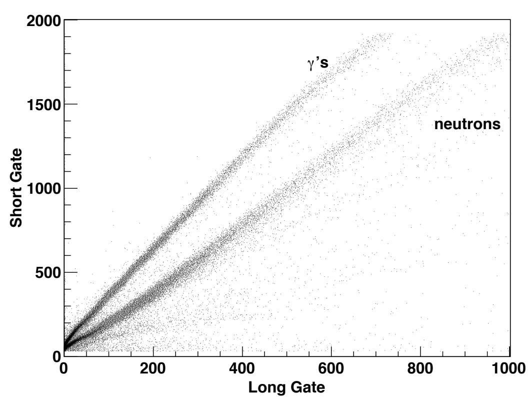

Figure 2: The fast vs. slow components of the scintillation pulse. The events due to the γ rays and neutrons interactions with the detector are the upper and lower curves, respectively.

figure. Near the lower limits of the fast and slow components, corresponding to γ-ray and neutron energies below around 120 keV and 1 MeV, respectively, the separation between particles is no longer distinguishable. Thus, both the TOF and the pulse-shaped discrimination (PSD) techniques were exploited to completely distinguish between the different types of particles. The spectra of the prompt neutrons and γ rays were analyzed separately and the analysis of the neutron distributions will be presented elsewhere. This manuscript will focus on the results from the γ-ray analysis.

3. Discussion

The distributions measured by any detector are always distorted by the detector response. Thus, one can mathematically represent a measured distribution $\mathbf{b}$ by a matrix equation $\mathbf{b}=\mathbf{A}\mathbf{x}$, where $\mathbf{A}$ is a two dimensional (2D) $m\times n$ sized smearing matrix whose elements are determined by the detector response and $\mathbf{x}$ is the incident distribution on the detector. In order to recover the distributions and energies of the incident particle, one must be able to solve the above equation for $\mathbf{x}$. In general if the incident distributions are distorted only by a single physical variable, one can solve for the true events through bin-to-bin correlations if the measured values are close to real ones, i.e the migration of events to the neighboring bins is negligible. If the measured values are not close to the real ones and the smearing matrix is nonsingular, one can try to invert the response matrix to recover the "true" distribution. In many cases, this method fails to handle large statistical fluctuations in the data and can give unstable results. Instead, in the current work, we choose to deduce the incident γ-ray distributions using the Single Value Decomposition (SVD) and the iterative Bayesian methods. In the SVD unfolding technique, the smearing matrix is factorized into a product of three 2D matrices, a $m\times m$ orthogonal times a nonnegative $m\times n$ diagonal times a $n\times n$ orthogonal one, in order to create a system of linear equations [20]. The eigenvalues and eigenvectors of the system can then be solved to determine the "true" distribution. In the iterative Bayesian technique, a statistical approach is used to deduce the "true" distribution, (see, for example, [21]). In this method, the number of events observed is written in terms of the summation of the product of the number of events from each effect (i.e. the incident γ rays) that caused the event times the probability from the smearing matrix that the observed event happens given that effect has occurred. The probabilities are weighted based on prior knowledge or assumed to be initially uniform if no previous information is known. The weighting factors are calculated iteratively using the values from the previous iteration until a "small" chi-squared is reached. A more comprehensive summary on the unfolding methods can be found in Ref. [22].

3.1. Detector Response

In order to build the Monte Carlo simulation of the smearing or detector response matrix, one needs to know the possible interaction mechanisms for photons in matter. The photoelectric effect is known to be the dominant photon interaction mechanism at relatively low energies. The cross section for the photoelectric effect process is approximately proportional to $Z^{4.5}$, where Z is the atomic number of the absorbing material [23]. This process is suppressed in liquid scintillators due to the low atomic numbers of the scintillation material, which is comprised of mostly carbon and hydrogen. Thus, a continuum due to the Compton scattering of the photons becomes the most likely process to be measured by the detector and makes identifying the incident photon energy more difficult. In order to reconstruct the "true" photon energies incident on a liquid scintillator, one must be able to reconstruct the physical interactions by accurately characterizing the detector response and understanding the light output collected by the photocathodes.

Extensive studies on the light output functions for charged particles in liquid scintillators such as the NE213 have been done (see, for example, [24]). For electrons with a kinetic energy above 50 keV, the light output is approximately proportional to the electron energy [25]. The inefficiency of collecting all the light from the ionization energy of the liquid (L) results in the deterioration in the detector resolution. Thus, the full width at half maximum (ΔL) of the integrated detector signal may be described by the resolution function:

$$\frac{\Delta L}{L} = \sqrt{\alpha^2 + \frac{\beta^2}{L} + \frac{\gamma^2}{L^2}}. \tag{1}$$

The resolution parameters α, β and γ, which arise from contributions due to the locus dependent light transmission from the detector to the photocathode, the statistical effects of the light production, attenuation, photon/electron conversion, amplification, and noise, respectively, are detector-dependent and must be determined experimentally.

The influence of the detector size, geometry and their contributions to the detector response were measured using a PuBe mixed neutron and γ-ray source and four standard calibration sources: ^{22}Na, ^{88}Y, ^{60}Co and ^{137}Cs. A large volume NaI(Tl) detector located approximately 30 cm away from the center of the source was used in coincidence with the liquid scintillators to measure the detector response spectra due to the ^{22}Na, ^{88}Y and ^{60}Co sources. These coincidence measurements provided cleaner spectra by reducing the random room background measured by the scintillators. A geometric model of the detector array including the PPAC and its environment was built into a GEANT4 [26] simulation to calculate the response of the liquid scintillators as a function of incident γ-ray energy. The measured pulse heights were aligned with the simulated spectra from GEANT4 to convert channel number into photon energy. The energy calibrations were found to be linearly dependent on the pulse height with fluctuations between the fit and the data as large as 3% at 2 MeV.

The high-energy side of the peaks due to multiple Compton scattering of the photons from four calibration sources, and the background lines at 1461 and 2615 keV was fitted with Gaussians to determine ΔL and the resolution parameters α, β and γ, see Fig 3. The resolution function with α, β and γ equal to 0.067, 0.21 and 0.11 respectively, has been observed to follow Eq. 1 and has a

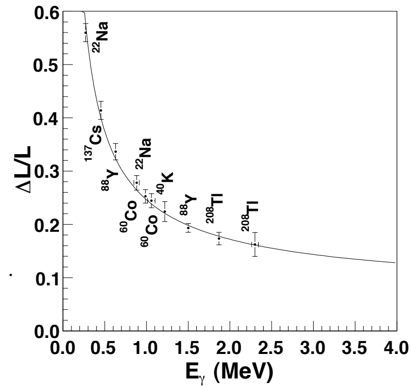

Figure 3: The relative detector resolution of the liquid scintillators vs. the centroid of a Gaussian. The solid curve is a fit to the data using Eq. 1.

similar β-to-α ratio of 3.5 as published in Ref. [25] for a larger 25.4 cm diameter detector. The response function near the upper limit of the pulse height spectrum was approximated using a Gaussian fall off whose width was established from the Compton scattering spectrum of the 4.4 MeV transition from the PuBe source. The values of the parameters from the fit were then implemented in the resolution function used in GEANT4 to build a response function of the γ-ray detector for incident photon energies up to 6 MeV. Response functions from random sampling of the γ-ray transitions in ^{22}Na and ^{88}Y using by their known intensities were generated by GEANT4 to determine the detector efficiency. Comparisons with measured background subtracted were done to validate the efficiency curve and were determined to have good agreement as seen in Fig. 4.

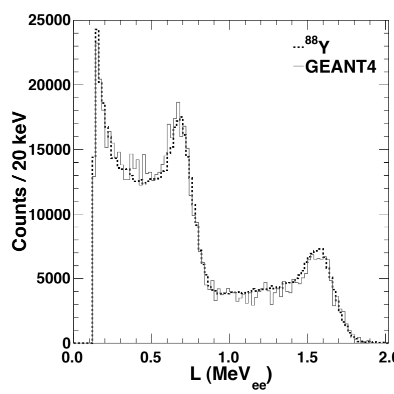

Figure 4: Validation of the detector efficiency from GEANT4 for the ^{88}Y transitions compared with the background subtracted measured spectrum (dashed histogram). The GEANT4 response curve was generated for a ^{88}Y source using γ-ray intensities from ENSDF [27].

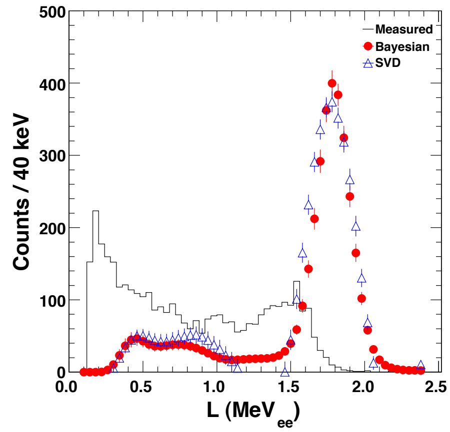

Figure 5: The measured spectrum of a ^{88}Y source in coincidence with the 898 keV transition measured by a NaI(Tl) detector. The filled circles denote the distribution deduced using the iterative Bayesian method, and the open triangles are the calculation using SVD.

3.2. Unfolding Calibration Sources

The unfolding matrix obtained using GEANT4 simulations was tested against the measured response functions of the calibration sources by using the SVD and iterative Bayesian algorithm in the RooUnfold package [28]. Shown in Fig. 5 is the measured distribution from a 10 μCi ^{88}Y due to the Compton scattering in the liquid scintillator detectors. The spectrum was obtained by using a coincidence gate around the 898 keV transition measured by the large volume NaI(Tl) detector. The filled circles and open triangles are the solutions for the incident γ-ray distribution determined using the Bayesian and SVD methods, respectively. Each technique shows a transition centered around 1800 keV corresponding to the 1836 keV transition in ^{88}Y, but the SVD method results in a slightly broader distribution with a ΔL of 337 keV compared to 306 keV from the Bayesian method. The uncertainties of the unfolding routines are determined using the diagonal of the covariance matrix but do not incorporate the $\sim$0.3% statistical uncertainties from the response matrix, see section 5.1 in Ref. [28] for more details. Despite background subtracting for the Compton events that result from higher incident γ-ray energies, the second bump due to events in coincidence with the Compton scattering of the 1836 keV transition in the NaI(Tl) within the 898 keV gate is still present.

3.3. Californium-252

To investigate whether it is possible to unfold the detector response of the liquid scintillators from a continuous energy distribution, the unfolding routines were tested using a measured spectrum from the spontaneous fission of ^{252}Cf, and the resulting unfolded distributions with the spectra obtained using other detector systems. Currently, there are only two known publications which contain the true incident γ-ray distribution up to 8 MeV and another two data sets up to 6 MeV. The first data set was taken using a single NaI(Tl) detector by Verbinski *et al* [14]. Structures at the low energy part of the γ ray distribution were observed before peaking at around 1 MeV. The distribution then drops nearly five orders of magnitude over the next 6.5 MeV. This general trend is consistent with the results from another experiment [29] using the 4π array of BaF_2 known as DANCE except at above 4 MeV, where a steeper drop in the γ-ray intensities has been observed.

Shown in Fig. 6(a) is the prompt γ-ray pulse height distribution for the spontaneous fission of ^{252}Cf measured in the current work. For the SVD technique, the number of degrees of freedom used in the unfolding matrix needed to be limited to approximately the number of bins in the observed spectrum. Thus, the response matrix was limited to incident γ-ray energies up to 5 MeV, see Fig. 7. The relative efficiency of the detector array is also projected on to the right side of the figure at $E_{response} = 4.94$ MeV. A larger response matrix with incident γ-ray energies up to 6 MeV was used for the iterative Bayesian technique. Both the Bayesian and SVD methods predict exponential decays with similar slopes above 1 MeV, but disagree below 1 MeV. The Bayesian method indicates that there is a broad peak in the distribution around 300 keV, while the SVD technique suggests a much broader and smoother curve.

Shown in Fig. 6(c) is the incident γ-ray distribution from the iterative Bayesian method compared to Ref.[14] and Ref. [29], the unfilled stars and circles, respectively. In Fig. 6(b) is a comparison of the unfolded γ-ray distribution from Ref. [30] measured by a NE213 organic scintillator using a Least-squares method. The distributions in Fig. 6(b-c) were normalized from $\sim$1.0-3.5 MeV by their total pulse height relative to the current work. If the distributions were unfolded correctly, one would expect to see similar distributions neglecting the fine features due to the different detector resolutions. The spectra measured by liquid scintillators detectors are consistent with each other below 3 MeV. The authors of Ref. [30] suggest that the oscillation above 4 MeV may be do to an artifact from their unfolding procedure. The distribution deduced from the current work using the Bayesian method has the similar trend to what was observed using the DANCE array, which had a 150 keV threshold. The different thresholds of the detector systems used to measure the distributions and the energy cutoff at higher energies in the current work caused the deviations at around 250 keV and 4.0 MeV, respectively. With the current setup, the measurement of the shape in the region above 4.5 MeV, where the slopes observed by Refs. [14] and [29] deviate, can not be deduced.

3.4. Uranium-235

There exist several published measurements of the total and/or average prompt γ-ray energies from the fission of the ^{235}U at incident neutron energies up to 15 MeV, see Refs. [31, 32], but there are only two published results to the best of our knowledge which give the γ-ray distributions emitted from fission. Both of these publications were neutron-induced fission taken at thermal

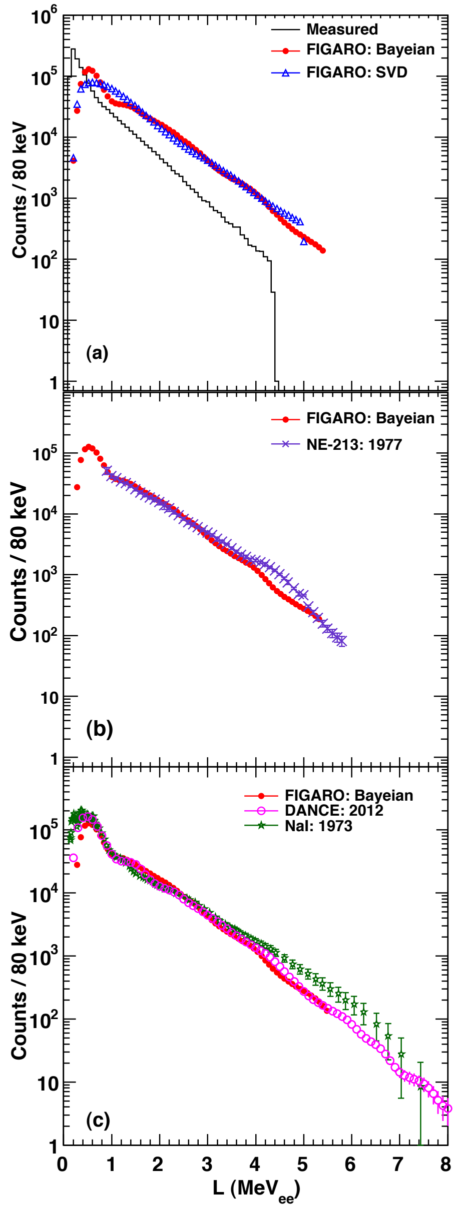

Figure 6: (a) The measured and unfolded pulse height spectra for the spontaneous fission of ^{252}Cf. The symbols retain their meaning from Fig. 5. (b) Comparisons of the Bayesian unfolded spectrum with the spectrum from Ref. [30], (c) Ref. [14], and the Bayesian unfolding spectrum from Ref. [29]

energies by Verbinski *et al*. [14] and by Peelle and Maienschein [33]. In addition, there also exist two Los Alamos Scientific Laboratory internal reports by

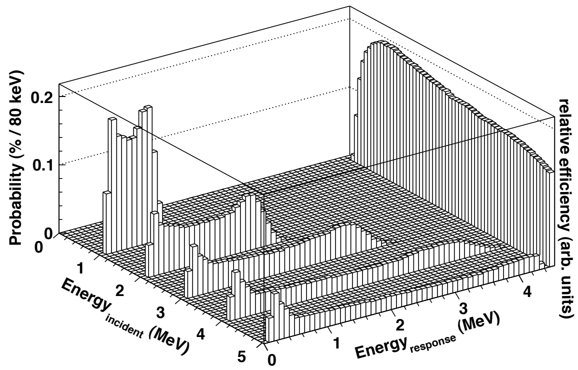

Figure 7: The detector response matrix simulated by GEANT4 for incident γ rays at 1, 2, 3, 4, and 5 MeV for the Chi-Nu array. The efficiency curve is projected on to the right side of the figure.

Drake measuring the distributions at incident energies of 1, 2, and 5 to 8 MeV in 500 keV steps [15, 16]. Using a single NaI(Tl) detector and a surface-barrier fission detector, Verbinski *et al*. deduced that on average 6.51(30) MeV in total photon energy ($< E_{\gamma}^{total} >$) is released per fission, where the average photon energy is approximately 0.97(5) MeV. The distribution from the thermal-induced fission determined by Verbinski *et al*. was observed to have a similar pattern to that seen in the spontaneous fission of ^{252}Cf for γ rays in energy range between 0.14 to $\sim$4 MeV. Peelle and Maienschein observed a similar unfolded distribution except at around 1.7 to 3.0 MeV where they observed slightly larger γ-ray intensities. From their distributions, they obtained an average photon energy of 7.18(26) MeV from thermal-induced fission which is greater than the total energy equal to 6.43(30) MeV obtained by Pleasonton *et al.* [34]. The latter is consistent with Verbinski *et al.*. Using a large gadolinium-loaded liquid scintillator, Frehaut *et al.* [32] measured the total photon energy from fission a function of the incident neutron energies from 1 to 15 MeV. The $< E_{\gamma}^{total} >$ was found to have a small but nearly linear increasing dependence on the incident neutron energy, see Ref. [35].

The prompt γ-ray distributions from ^{235}U were measured at neutron incident energies from 1.0 to 20.0 MeV in the current work to study the effect of the bombarding energy on the shape of the distributions. By validating the unfolding techniques used in the current work against the γ-ray distributions from calibration sources and the spontaneous fission of ^{252}Cf, we were convinced that we can use the same methods to deduce the γ-ray distributions from fission of other nuclei. The γ-ray events from the neutron-induced fission of ^{235}U within $\pm$ 6 ns of the time difference between the liquid scintillator and the PPAC were examined at three different incident neutron energy ranges: 1-2, 5-10, and 10-20 MeV. The incident energy ranges were chosen based on regions where single or multi-chance fission are known to occur.

Figs 8(a)-(c) are comparisons of the pulse height distribution for the prompt γ rays as a function of the γ-ray energy for neutron incident energies of 1-2, 5-10 and 10-20 MeV, respectively. All events detected by the six chosen liquid scintillator detectors were summed for statistical purposes; thus any anisotropy due to the angular distributions was neglected. The distributions were unfolded using a response matrix generated from GEANT4 for incident γ-ray energies up to 5 MeV. The incident spectra deduced from the two unfolding techniques, the iterative Bayesian and SVD are essentially identical above 1.8 MeV. The uncertainties from the unfolding routines are again calculated using the covariance matrix and increase from $\sim$3% at 500 keV to $\sim$10% at 4 MeV. Comparisons with the distributions from Refs. [14, 15] at thermal and 1 MeV incident energies and Ref. [16] at bombarding 5 MeV are also included in panels (a) and (b), respectively. A general agreement from all the experiments can be seen from γ-ray energies between 1 to 4 MeV and the disagreement below 800 keV is due to the threshold at 130 keV in the current experiment. Shown in panel (d) is the spectra for the three energy ranges obtained using the iterative Bayesian method normalized to the spectrum in (b). The three γ-ray distributions in panels (a) through (c) obtained using the iterative Bayesian and SVD methods have essentially the same shape within uncertainties. This suggests that the temperature of the fission fragments after neutron evaporation may be independent of the incident bombarding neutron energy.

In the comparison of the prompt γ-ray distributions from the spontaneous fission of ^{252}Cf and the thermal-neutron-induced fission of ^{235}U, Verbinski *et al.* found a systematic softening of the γ-ray spectra with increasing mass number of the fissioning isotope. A comparison of the distributions from the current work for the prompt γ rays from fission of ^{235}U and ^{252}Cf is given in Fig. 9. The distribution from the spontaneous fission of ^{252}Cf has been normalized to the distribution from the neutron-induced fission ^{235}U from $\sim$1-4MeV for the purpose of comparison. The variations in the end points of the distributions arise from the differences in the measured statistics at around 4 MeV.

Except for the fine details in the californium distribution, both distributions have the same monotonically decreasing trend with approximately the same slope in the energy region from 1 to 4 MeV. Future measurements with improved statistics will be carried out using ^{235}U and ^{239}Pu targets to measure the distributions past 4 MeV to determine if the softening at the higher γ-ray energies observed by Verbinski *et al.* is a global feature for neutron-induced fission.

4. Summary

Two experiments measuring the prompt γ-ray distributions from the spontaneous fission of ^{252}Cf and neutron-induced fission of ^{235}U were carried out at LANSCE using the FIGARO neutron array. Unfolding was performed for the fission γ-ray distributions measured with liquid scintillators by the SVD and iterative Bayesian techniques that were validated using calibration sources and comparing with previous measurement on the spontaneous fission of ^{252}Cf. The iterative Bayesian method is able to reproduce the finer details observed in other measurements while the SVD approach yields a broader distribution and smoothes any fine details. The same monotonically decreasing slope was observed for the γ-ray energies from 1.0 to 4.0 MeV for ^{252}Cf and the ^{235}U regardless of neutron incident energy. Future measurements are planned to extend the distributions past 4 MeV with markedly improved statistics thus allowing the structure of the distribution to be investigated. The success of using the modern unfolding techniques to unfold the γ-ray distributions from fission with a liquid scintillator array will pave the way for future studies on γ-neutron correlations needed to improve the predictive capabilities for neutron and γ ray emissions in fission models.

Acknowledgements

This work benefited from the use of the LANSCE accelerator facility and was performed under the auspices of the U.S. Department of Energy by Lawrence Livermore National Laboratory under Contract DE-AC52-07NA27344 and Los Alamos National Laboratory under Contract DE-AC52-06NA25396.

References

[1] R. A. Knief, Nuclear Engineering Theory and Technology of Commercial Nuclear Power, 2nd edition, Taylor & Francis, 1992, pp. 46

[2] A. Lüthi, Ph.D. thesis, École Polytechnique Fédérale de Lausanne (1998)

[3] D. Blanchet, N. Huot, P. Sireta, H. Serviere,M. Boyard,M. Antony, V. Laval, P. Henrard, Annals of Nuclear Energy 35 (2008) 731

[4] G. Rimpault, in: P. Rullhusen (Ed.), Proceedings of the Workshop on Nuclear Data for Generation IV, Antwerpen, Belgium, April 5-7, 2005, European Commission, Joint Research Centre, Institute for Reference Materials and Measurement, World Scientific Publishing Co., 2006, pp. 18

[5] A. J. Koning, S. Hilaire, M. C. Duijvestijn, Talys-1.0, in: O. Bersillon, F. Gunsing, E. Bauge, R. Jacqmin, S. Leray (Eds.), Proceedings in International Conference on Nuclear Data for Science and Technology, Nice, France, April 22-27, 2007, Commissariat à l'Énergie Atomique, EDP Sciences, 2008, pp. 211

[6] M. Herman, R. Capote, B. V. Carlson, P. Oblozinsky, M. Sin, A. Trkov, H. Wienke, V. Zerkin, EMPIRE: Nuclear reaction model code system for data evaluation, Nucl. Data Sheets 108 (2007) 2655

[7] D. T. Hughes, R. B. Schwartz, Brookhaven National Laboratory Report No. 35, 1958 (unpublished)

[8] M. B. Chadwick, P. Obložinský, M. Herman, N. M. Greene, R. D. McKnight, D. L. Smith, P. G. Young, *et al.*, ENDF/B-VII.0: Next generation evaluated nuclear data library for nuclear science and technology, Nucl. Data Sheet 107 (2006) 2931, and references therein.

[9] T. Ethvignot, M. Devlin, H. Duarte, T. Granier, R. C. Haight, B. Morillon, R. O. Nelson, J. M. ODonnell, D. Rochman, Phys. Rev. Lett. 94 (2005) 052701

[10] S. Noda, R. C. Haight, R. O. Nelson, M. Devlin, J. M. ODonnell, Phys. Rev. C 83 (2011) 034604, and references therein

[11] P. Staples, J. J. Egan, G. H. R. Kegel, A. Mittler, M. L. Woodring, Nucl. Phys. A 591 (1995) 41

[12] G. S. Boykov, V. D. Dmitriev, G. A. Kudyaev, Y. B. Ostapenko, M. I. Svirin, G. N. Smirenkin, Yad. Fiz. 53 (1991) 628

[13] N. Kornilov, Prompt fission neutron spectra of major actinide, international Nuclear Data Committee report INDC(NDS)-0571 (2010)

[14] V. V. Verbinski, H. Weber, R. E. Sund, Phys. Rev. C 7 (1973) 1173

[15] D. M. Drake, Los Alamos Scientific Laboratory Report No. LA-5048, 1972

[16] D. M. Drake, Los Alamos Scientific Laboratory Report No. LA-5134, 1973

[17] R. C. Haight, J. M. ODonnell, L. Zanini, M. Devlin, D. Rochman, in: J. Kvasil, P. Cejnar, M. Krticka (Eds.), Proceedings in the Capture Gamma-Ray Spectroscopy and Related Topics, Pruhonice, Prague, Czech Republic, September 2-6, 2002, Charles University, Prague, Czech Republic, World Scientific Publishing Co., 2003, pp. 451

[18] C. Y. Wu, R. Henderson, J. Gostic, R. C. Haight, H. Y. Lee, Lawrence Livermore National Laboratory LLNL-TR- 461044, 2010

[19] R. A. Henderson, J. M. Gostic, J. T. Burke, S. E. Fisher, C. Y. Wu, Nucl. Instr. and Meth. A 655 (2011) 66

[20] A. Höcker, V. Kartvelishvili, Nucl. Instr. and Meth. A 372 (1996) 469

[21] G. DAgostini, Nucl. Instr. and Meth. A 362 (1995) 487

[22] G. Cowan, Statistical Data Analysis, Oxford University Press, 1998

[23] G. F. Knoll, Radiation Detection and Measurement, 3rd edition, John Wiley and Sons, New York, 1994

[24] V. V. Verbinski, W. R. Burrus, T. A. Love, W. Zobel, N. W. Hill, R. Textor, Nucl. Instr. and Meth. 65 (1968) 8

[25] G. Dietze, H. Klein, Nucl. Instr. and Meth. 193 (1982) 549

[26] S. Agostinelli, J. Allison, K. Amako, J. Apostolakis, H. Araujo, P. Arce, M. Asai, *et al.*, Nucl. Instrum. Meth. A 506 (2003) 250

[27] G. Mukherjee and A. A. Sonzogni, Nucl. Data Sheets 105 (2005) 419

[28] T. Adye, ArXiv:phyics.data-an/1105.1160v1

[29] A. Chyzh, C. Y. Wu, E. Kwan, R. A. Henderson, J. M. Gostic, T. A. Bredeweg, **et al.**, Phy. Rev. C 85 (2012) 021601(R)

[30] D. T. Ingersoll and B. W. Wehring, Nucl. Instrum. Meth. 147 (1977) 551

[31] T. E. Valentine, Annals of Nuclear Energy 28 (2001) 191

[32] J. Fréhaut, A. Bertin, R. Bois, in: K. H. Boeckhoff (Ed.), Proceedings of the International Conference on Nuclear Data for Science and Technology, Antwerp, Belgium, September 6-10, 1982, Reidel, Dordrecht, The Netherlands, 1983, pp. 78

[33] R. W. Peelle, F. C. Maienschein, Phys. Rev. C 3 (1971) 373

[34] F. Pleasonton, R. L. Ferguson, H. W. Schmitt, Phys. Rev. C 6 (1972) 1023

[35] D. G. Madland, Nucl. Phys. A 772 (2006) 113

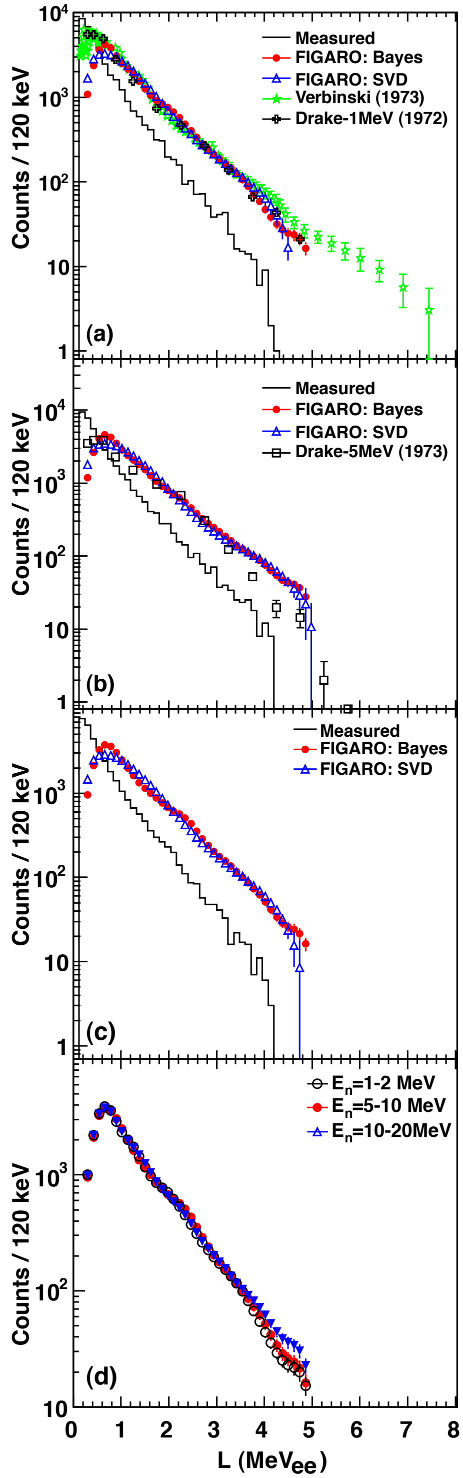

Figure 8: The measured and unfolded pulse height spectra by liquid scintillators for the neutron-induced fission of ^{235}U at projectile energies of (a) 1 to 2, (b) 5 to 10 and (c) 10 to 20 MeV. The symbols retain their meaning from Fig. 5. The distributions from Refs.[14, 15] and Ref. [16] are also plotted in panels (a) and (b), respectively, for comparison. (d) The normalized pulse height spectra unfolded using the iterative Bayesian method.

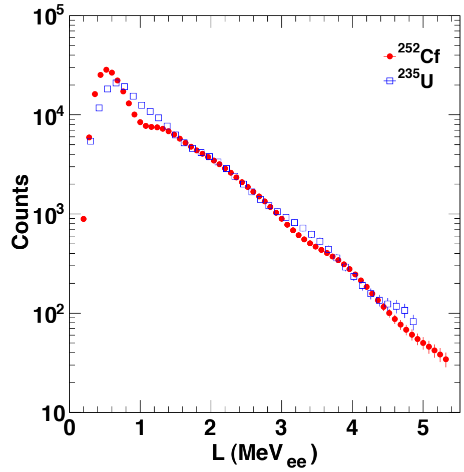

Figure 9: Comparison of the unfolded pulse heights spectra using the iterative Bayesian method for the neutron-induced fission of ^{235}U at projectile energies of 1.0 to 2.0 MeV, and the spontaneous fission of ^{252}Cf.